Planar Laser-Induced Iodine Fluorescence Technique for Flow Visualization and Quantitative Measurements in Rarefied Flows

Professor James McDaniel*, Eric Cecil*, Erin Reed* and Josh Codoni*
Professor Iain Boyd¶ and Hicham Alkandry¶

*Department of Mechanical and Aerospace Engineering, University of Virginia, Charlottesville, VA 22904
¶Department of Aerospace Engineering, University of Michigan, Ann Arbor, MI 48109

Abstract: Planar Laser-Induced Iodine Fluorescence (PLIIF) is a powerful nonintrusive technique for flow visualization and quantitative measurements in continuum and rarefied flows. The technique provides measurements of multiple flowfield parameters in a cross-sectional plan of the flow. A theoretical model of the PLIIF is given, followed by details of the experiments, results and comparison with calculations.

INTRODUCTION

Figure 1 is an energy level diagram of the iodine molecule. Iodine is excited from the v"=0 ground electronic X state to the excited B state. The excited molecules relax to the ground state through radiative emission, fluorescence; however, collisional quenching competes with the radiative emission and reduces the fluorescence emission.

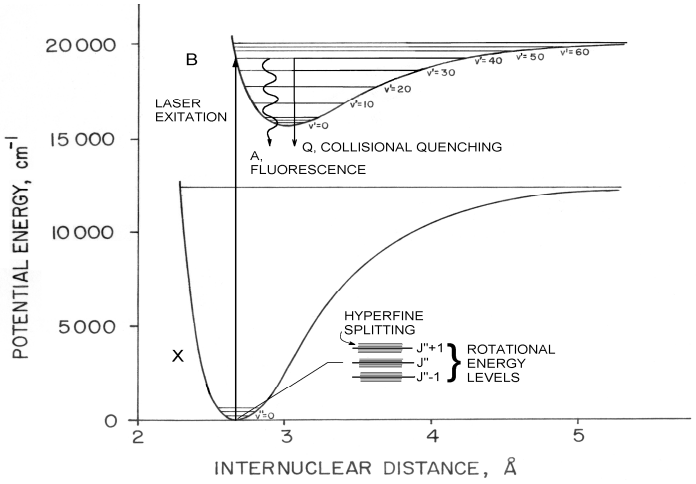

Figure 1: Iodine energy level diagram

The rate equation solution for the fluorescence signal of a single transition is given in the equation below:

$$S_F = C f_1(T) \frac{A_{21}}{A_{21} + Q(p,T)} \frac{1}{\Delta \nu_D} V(p,T,u) I(x) f_s N$$

The first term in this equation, f_1 is the Boltzmann population fraction of the vibrational/rotational energy level being excited by the laser; the next term is the ratio of the radiative emission rate to the total relaxation rate (termed the Stern-Volmer fraction); the Voigt function (V) gives the transition lineshape; I

is the laser intensity; f_s is the iodine seeding fraction; and N is the flowfield number density. It is seen that the fluorescence signal is a complex function of the gas temperature, pressure and flow velocity. Although this makes the interpretation of the signal less than straightforward, it illustrates that the signal is rich in thermodynamic properties and convective and thermal velocity and, if these can be isolated, would result in the measurement of multiple flowfield properties.

The Boltzmann population fraction is given as the product of the rotational and vibrational fractions, where thermal equilibrium is assumed. The primary absorption lines under the argon laser gain profile at 514.5nm are in the ground vibrational state, v"=0, which is strongly populated at room temperature and below. The low rotational quantum numbers, 13 and 15, of these transitions produce large rotational population fractions at temperatures below room temperature. In fact, it is these low rotational quantum numbers that make the PLIIF technique so powerful in the supersonic and hypersonic flow regimes. The Stern-Volmer fraction represents the fraction of the excited state population that decays due to radiation, A_{21}, versus collisional quenching, Q(p,T). At high Mach numbers, the collisional quenching rate becomes small compared to the radiative decay rate and the Stern-Volmer fraction approaches unity. This greatly simplifies the interpretation of the fluorescence signal in the rarefied, hypersonic regime. The broadening of the absorption lines is represented by the Voigt lineshape function. This function is a convolution of Doppler broadening and Lorentz broadening.

EXPERIMENTAL APPROACH

Hypersonic Flow Facility and Optical Setup

The flow facility is provided by evacuating a vacuum chamber and introducting iodine-seeded nitrogen through a sonic nozzle. The resulting flowfield is an underexpanded jet. The jet is physically about 4 inches in length from the sonic exit to the Mach disk. The variation of Mach number and Knudsen number in the underexpanded jet is shown in Figure 2.

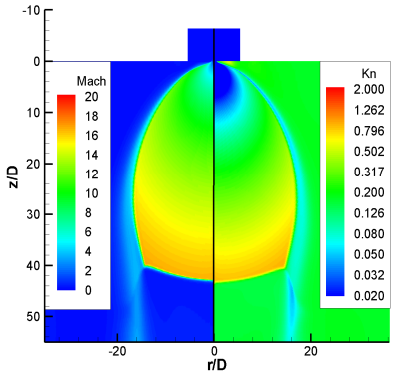

Figure 2: Mach and Knudsen number variation in underexpanded jet flow facility.

It is seen in figure 2 that the Mach number ranges from 1 at the sonic exit to about 16 at the Mach disk location, while the Knudsen number ranges from about 0.02 to 1 over the same range. Models are placed in the underexpanded jet test flow at locations which give the desired Mach number for the tests, according to Method of Characteristics calculation of the flowfield. Note that the streamlines for the tests are not parallel, but diverge from the exit source flow.

The optical setup for the experiment is shown in Figure 3. The output from the laser is converted into a thin laser sheet. This sheet is passed through the plane of the model (flat plate model shown). The resulting fluorescence image is collected at 90 degrees using the CCD camera. The spectrum analyzer and static cell are used to monitor the frequency of the laser as it is tuned across the iodine absorption spectrum.

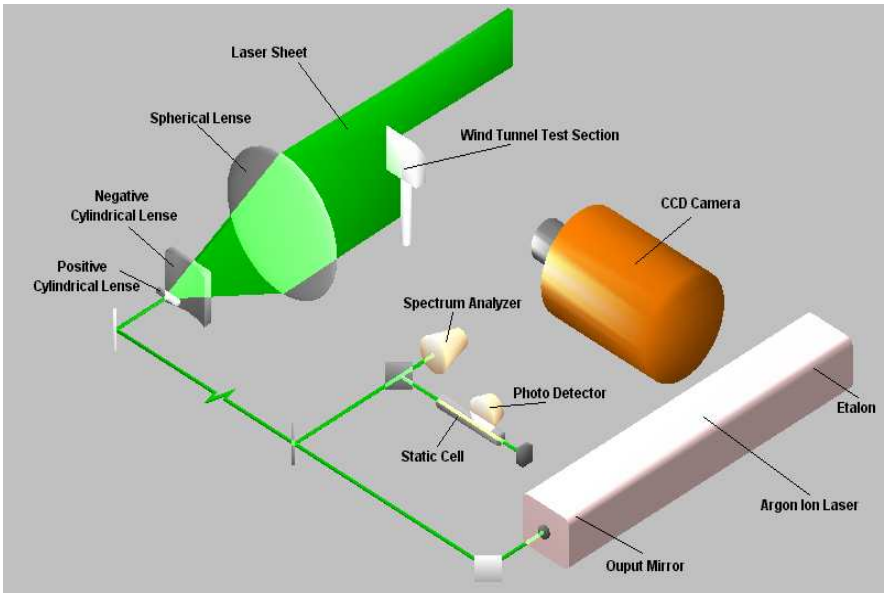

Figure 3: Optical setup for PLIIF technique

Narrowband measurement technique

When the linewidth of the exciting laser is less that the iodine transition linewidth, the fluorescence is given by the equation above. This equation describes the iodine absorption profile from a single transition. Actually there are multiple hyperfine components under the v"=0, J"=13 and 15 lines. Figure 4 shows the resolved hyperfine components of the absorption profile, as they appear at rarefied conditions.

For this narrow bandwith approach, the laser is tuned in frequency across the hyperfine components shown in Figure 4. At each discrete frequency, a fluorescence image is acquired using the CCD camera. Once this data is acquired, the absorption spectra at each pixel, corresponding to a discrete point in the flowfield, is reconstructed by looking at the same frequency in all the images. The resolved spectrum is fit by the theoretical model to obtain the flowfield parameters. The velocity is obtained by the Doppler shift of the absorption spectra, relative to the spectrum in a low pressure static cell. The rotational temperature is determined by the relative peak heights of the transitions, while the translational temperature is obtained from the Doppler-broadened line widths. Nonequilibrium between the translational and rotational temperatures can therefore be examined.

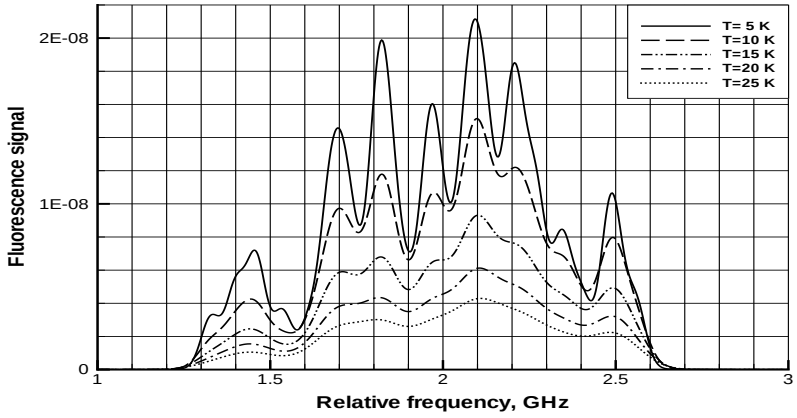

Figure 4: Iodine hyperfine components in rarefied conditions

Broadband measurement technique

When the linewidth of the exciting laser is greater that the iodine transition linewidth, the fluorescence is given by the equation below. In this case, the Voigt function is integrated to unity, since it is normalized, and the equation for the fluorescence simplifies so that only the Boltzmann fraction and the Stern Volmer fraction appear to modify the flowfield number density.

$$S_F = C\frac{A}{A+Q}f_1(T)n$$

For this technique, quantitative measurement of flowfield parameters is, in general, not possible since the absorption spectrum is not resolved. This approach is therefore a flow visualization technique. However, in the rarefied regime the fluorescence signal is proportional to flowfield number density. A plot of the Boltzmann fraction as a function of Mach number from an isentropic expansion in an underexpanded jet with a stagnation temperature of 300K is given in Figure 5. Note that the fraction becomes nearly constant for the J"=13, 15 transitions for Mach numbers in the 8 – 17 flow regime.

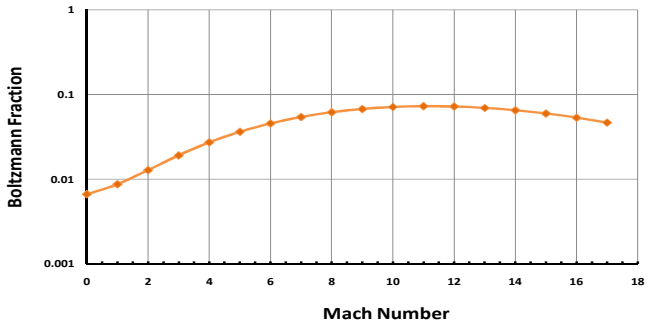

Figure 5: Boltzmann fraction vs Mach number in an isentropic expansion

A plot of the Stern-Volmer, or fluorescence efficiency factor, versus Mach number for the same isentropic expansion is given in figure 6. Note that the Stern-Volmer fraction becomes constant at unity for Mach numbers greater than about 8. This is to be expected since the collisional quenching rate is negligible under these conditions. Therefore, according to the equation for the broadband fluorescence, the signal should be directly proportional to the flowfield density in the rarefied regime above about Mach 8. This will be verified by experimental results given below.

RESULTS

The first results to be presented are narrowband measurements of the velocity field over a flat plate at a freestream Mach number of 12 (figure 7). The plate extends from X/D of 0 to 40. Note the divergent streamlines of the underexpanded jet test gas and the variation of velocity from about 760 m/sec in the freestream to near stagnation conditions at the trailing edge of the plate.

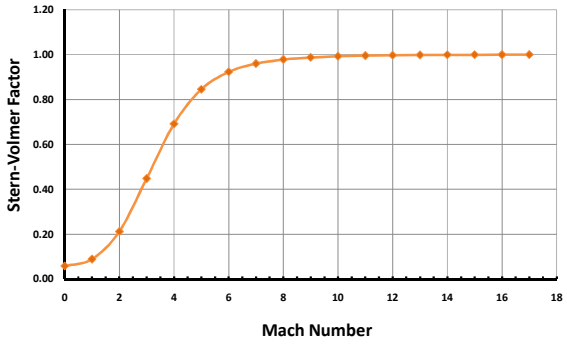

Figure 6: Stern-Volmer factor vs Mach number in an isentropic expansion

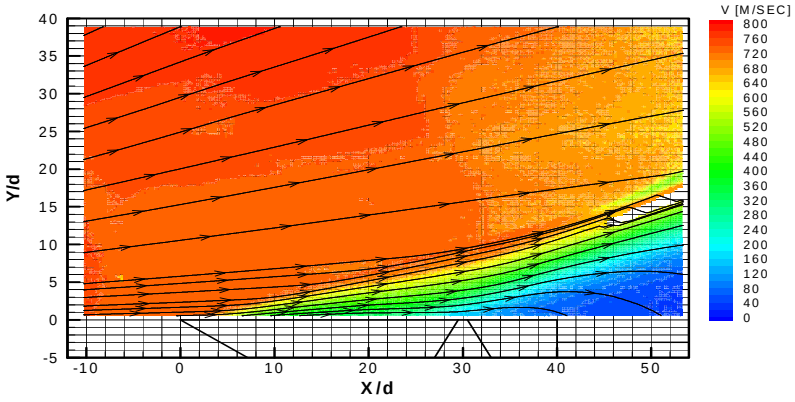

Figure 7: Velocity field for Mach 12 flow over a flat plate

The velocity profiles perpendicular to the plate are shown in Figure 8. Note the slip velocity is about 550 m/sec at the plate leading edge, where the boundary/shock layer is rarefied, to about 100 m/sec in the continuum region at the plate trailing edge.

Figure 9 gives the velocity field over the flat plate with a normal sonic jet, simulating a reaction control jet. The interaction of the normal jet with the hypersonic freestream is well resolved. Stagnation regions are seen ahead of and behind the transverse jet. A vortical region ahead of the jet is indicative of the horseshoe vortex that exists on the wall around the jet.

Broadband images for the injection of a reaction control system jet on a Mars Science Lab model at a Mach 12 freestream and angle of attack of 20 degrees are given in figure 10. The increase in jet size with increasing thrust coefficient is evident. These images clearly show the bow shock on the MSL forebody, the expansion around the shoulder and the interaction with the RCS jet.

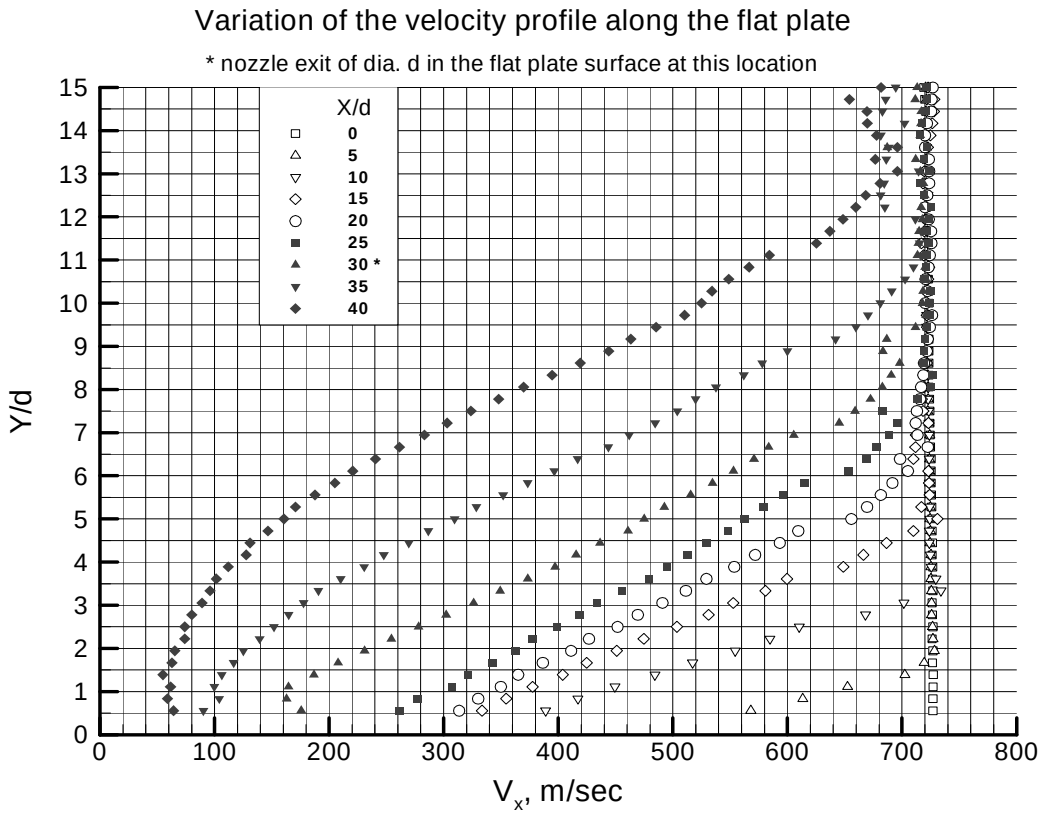

Figure 8: Velocity profiles normal to flate plate at Mach 12

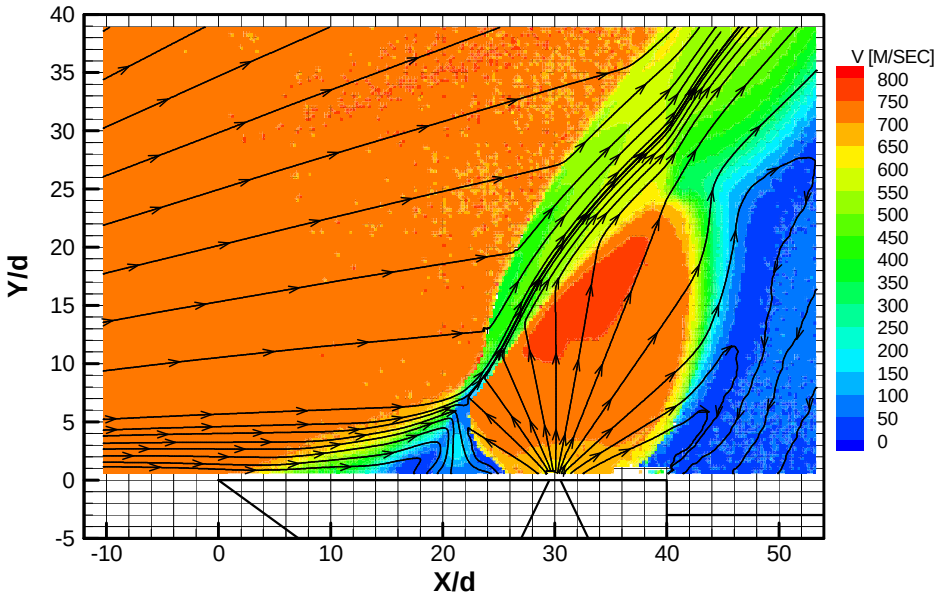

Figure 9: Velocity field for flow over a reaction control system jet

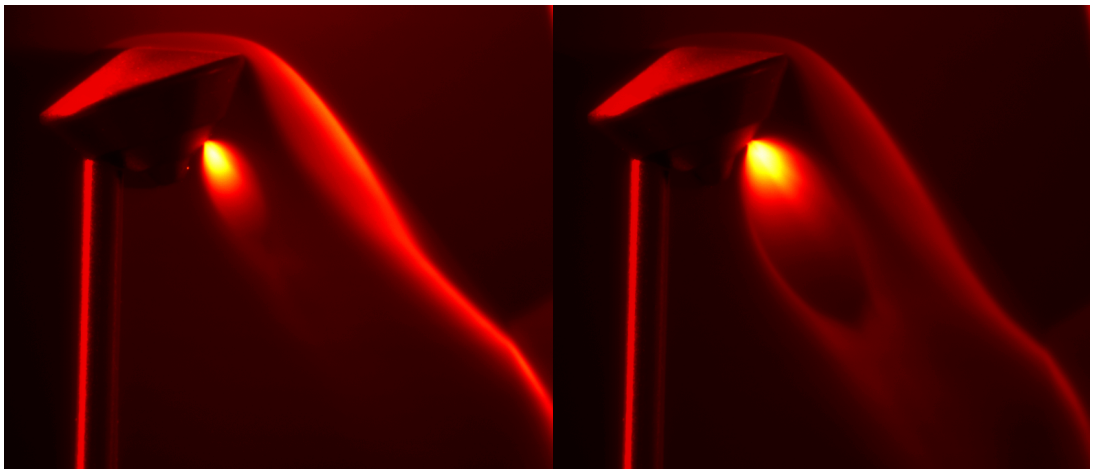

Figure 10: RCS injection on MSL. a) Thrust coefficient of 0.5 and b) 1.0.

A plot of the experimental data along the centerline of the RCS in figure 10 is given in figure 11. Note that the agreement of the experimental data with the broadband fluorescence equation is excellent. Near the jet exit the flow is continuum and the signal increases along the jet centerline owing both to the large increase in the Boltzmann population fraction and in the Stern-Volmer fraction (see figures 5 and 6). As the flow becomes rarefied, the Boltzmann population fraction becomes nearly constant and the Stern-Volmer fraction becomes constant at unity. In this regime, above about Mach 8, the broadband fluorescence signal is directly proportional to flowfield density, as discussed above. In most of the images shown in figure 10, this is the case, and the flow visualizational images are nearly quantitative.

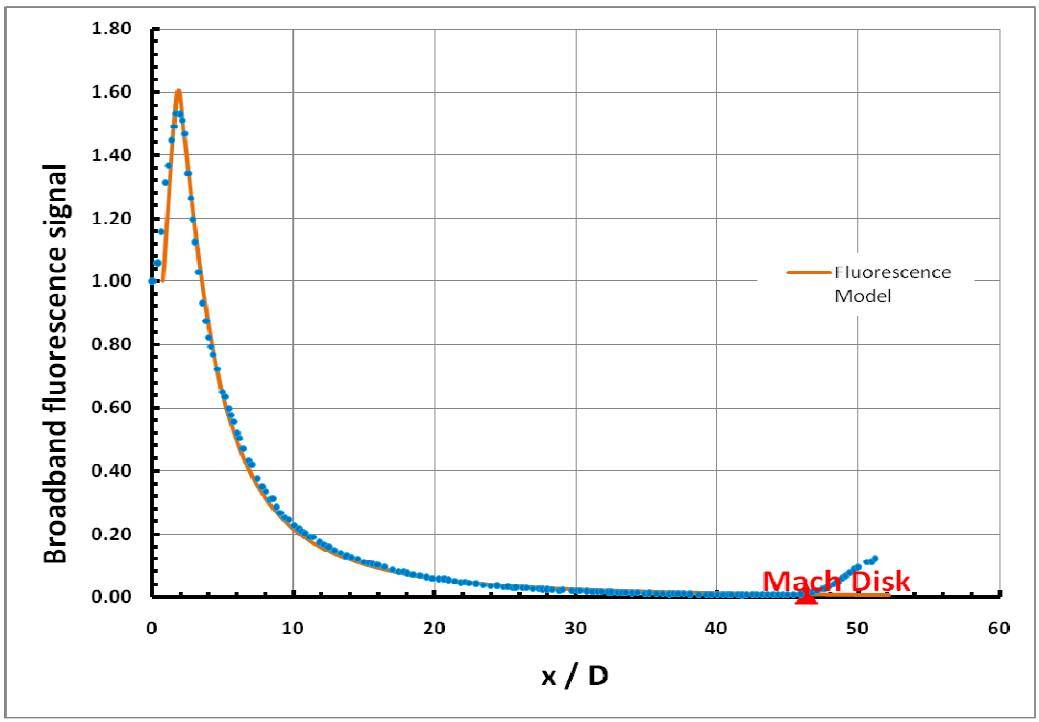

Figure 11: Variation of broadband fluorescence along centerline of RCS jet in figure 10.

These experiments are done in collaboration with computations at the University of Michigan. The calculations are done with a Navier-Stokes solver, LeMANS, which contains the capability for thermochemical nonequilibrium. When the gradient Knudsen number is greater than about 0.5, the flow experiences continuum breakdown and must be considered to be rarefied. Figure 12a shows that a considerable region of the flow on the lee side of the MSL at 20 degree angle of attack and Mach 12 is rarefied. The need to develop a hybrid CFD/DSMC computational method may be necessary to compute this entire flowfield. Figure 12b is a comparison of the LeMANS calculation of the streamlines of the RCS on the MSL with the broadband fluorescence image. Good agreement is seen for the bow shock on the MSL, but the expansion of the RCS jet seems to be overpredicted by the computation.

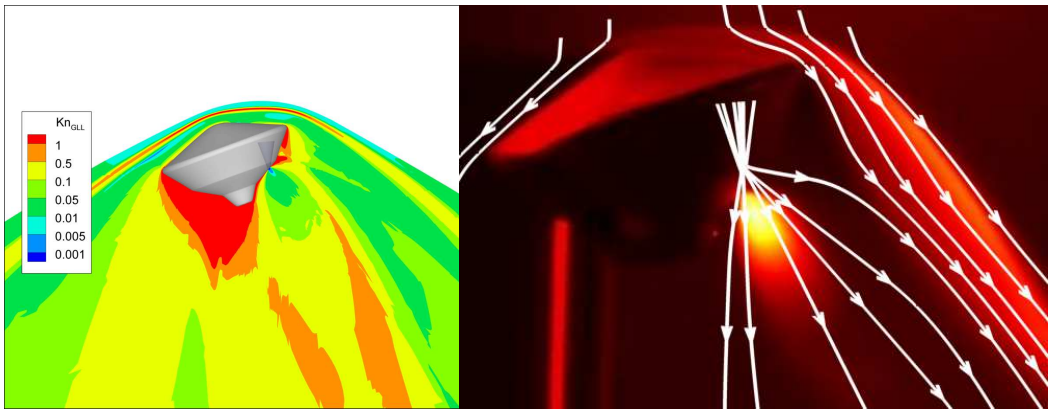

Figure 12: a) Mach 12 flow over MSL at 20 degree angle of attack b) calculated streamlines of RCS on MSL compared with fluorescence image.

CONCLUSION

The PLIIF technique has been presented from a theoretical basis, the experimental setup was discussed, and the two techniques techniques were presented. Results from quantitative velocity measurements of the Mach 12 flow over a flat plate and over a transverse RCS jet normal to the plate were shown. Flow visualization images were shown of a RCS jet firing from a Mars Science Lab model. The variation of the broadband fluorescence signal along the RCS jet centerline showed excellent agreement of the theoretical model with the experimental data. This comparison indicated that the broadband images are quantitatively proportional to flow density above about Mach 8. Computational results for the Knudsen number showed regions of continuum breakdown. Both the quantitative and qualitative measurements are important for validating computational methods being developed for these complex, continuum/rarefied flowfields.

ACKNOWLEDGEMENT

This research is supported at the University of Virginia and at the University of Michigan by NASA NRA grant NNX08AH37A. The technical monitor is Brian Palaszewski at the NASA Glenn Research Center.